Molecular Crystals and Liquid Crystals
Publication details, including instructions for authors and subscription information:
http://www.tandfonline.com/loi/gmcl20

Effect of Substituents on Electronic Spectral Shifts and Phase Stability of Liquid Crystalline Biphenylcyclohexane Molecules—A Theoretical Approach

P. Lakshmi Praveen [a] & Durga P. Ojha [a]
[a] Liquid Crystal Research Laboratory, Post-Graduate Department of Physics, Andhra Loyola College, Vijayawada, India

Available online: 20 Mar 2012

To cite this article: P. Lakshmi Praveen & Durga P. Ojha (2012): Effect of Substituents on Electronic Spectral Shifts and Phase Stability of Liquid Crystalline Biphenylcyclohexane Molecules—A Theoretical Approach, Molecular Crystals and Liquid Crystals, 557:1, 206-216

To link to this article: http://dx.doi.org/10.1080/15421406.2011.652849

Mol. Cryst. Liq. Cryst., Vol. 557: pp. 206–216, 2012

ISSN: 1542-1406 print/1563-5287 online
DOI: 10.1080/15421406.2011.652849

Taylor & Francis
Taylor & Francis Group

Effect of Substituents on Electronic Spectral Shifts and Phase Stability of Liquid Crystalline Biphenylcyclohexane Molecules—A Theoretical Approach

P. LAKSHMI PRAVEEN AND DURGA P. OJHA*

Liquid Crystal Research Laboratory, Post-Graduate Department of Physics, Andhra Loyola College, Vijayawada, India

The structures of liquid crystalline disubstituted biphenylcyclohexanes (BCHs) of the general formula R-C_6H_{10}-C_6H_4-C_6H_4-X with R: C_3H_7; X: H (BCH30), and R: C_5H_{11}; X: CN (BCH5CN) have been optimized using the density function B3LYP with 6–31+G (d) basis set using crystallographic geometry as input. Using the optimized geometry, electronic structures of the molecules have been evaluated using the density functional theory (DFT) calculations. Mulliken atomic charges for each molecule have been compared with Loewdin atomic charges to understand the molecular charge distribution and phase stability. The electronic absorption spectra and circular dichroism (CD) spectra of BCH molecules have been simulated by employing the DFT method. The excited states have been calculated via configuration interaction single level (CIS) with semiempirical Hamiltonian ZINDO. Two types of calculations have been performed for model systems containing single and double molecules of BCHs. Further, the spectra have been reported for all single molecules, and the ultraviolet (UV) stability of the molecules has been discussed. The stacked and in-plane dimer complexes have also been reported to enable the comparison between single and double molecules.

Keywords Electronic spectra; oscillator strength; phase stability

Introduction

The search for advanced materials with potential technological applicability has activated interest in electronic transitions and spectral shifts of liquid crystal (LC) compounds. These systems are considered as targets in materials science not only because of their unique physicochemical properties, such as chemical flexibility [1], phase stability [2], semiconductor behavior [3], and intense nonlinear-optical responses [4], but also due to their intrinsic capability of self-organization [5]. The interpretation of physical measurements on LCs requires a suitable theory [6, 7] for the response being measured in terms of observables. The molecular level approaches are often functional to assist in this issue, which can model observable properties making assumptions about molecular interactions and properties. Ultimately, the success of these theories should be the forecast of macroscopic properties from the geometric structure of constituent molecules.

*Address correspondence to Durga P. Ojha, Liquid Crystal Research Laboratory, Post-Graduate Department of Physics, Andhra Loyola College, Vijayawada 520008, India. E-mail: durga_ojha@hotmail.com

Optical features in the ultraviolet-visible (UV-Vis.) region can often be traced to the excitation of specific types of electrons in a material. Since most LC compounds contain an extended conjugated aromatic moiety, spectroscopic measurements, such as UV-Vis. absorption, are considered to be necessary [8], which influence the desired electronic or optical properties in the bulk phases of materials. Usually, this is monitored by UV-Vis. spectroscopy at the absorption maxima, which implies a destructive read-out of molecular systems. Hence, it is necessary to identify the molecular structures that can withstand a longer UV exposure. However, in most cases, the resulted spectra are not sufficient in exploiting them for practical purposes because of saturated absorption. In view of this circular dichroism (CD), measurements are taken for a better understanding of interaction of light with molecules in the UV-Vis. region [9, 10].

However, as the aromatic rings are the key components in determining the phase structure and properties, intermolecular interactions between the molecules have to be taken into account. The investigations of the phase behavior with regard to electronic structure of molecules, in particular, during the different modes of molecular interactions are still sparse. Such interactions can change the spectroscopic properties of the material and, typically, also suppress the overall response of the system [11]. Further, these effects are mainly severe for high-dipole-moment chromophores, and hence to predict their effect on the response of the material system is of great importance, especially in case of nonlinear optical materials [12].

The calculation of UV-Vis. spectra by computational chemistry tools is particularly appealing since the modern approaches are able to provide results with accuracy comparable to that obtained by experiments. In view of this, methods based on Time Dependent Density Functional Theory (TD-DFT) provide very accurate results [9, 13, 14]. Such approaches allow for the calculation of electronic transitions between the ground state and the different excited states, which give the energies of the corresponding radiations. Since electronic excitation processes involve an interaction of the charged electron with the fluctuating electric field of the electromagnetic radiation, it is expected that the absorption depends on common localization properties of these wavefunctions. For a given excitation, the transition probability is usually characterized by the oscillator strength [15] that is related to the integrated intensity of an absorption band. The macroscopic expression for the extinction coefficient can be deduced from the square of the transition moment on a microscopic level [16].

The present article deals with the UV-Vis. spectra and CD spectra of BCH30 and BCH5CN molecules. The highest occupied molecular orbital (HOMO) and the lowest unoccupied molecular orbital (LUMO) energies, absorption wavelength, oscillator strength (f), vertical excitation energies, and dipole moments have been reported. Further, an attempt has been made to explain the UV stability of systems based on the parameters introduced in this article. An examination of thermodynamic data has revealed that BCH30 exhibits a smectic B-isotropic transition at 366 K, and BCH5CN exhibits a nematic-isotropic transition temperature at 494 K [17].

Computational Methodology

The wavefunctions of the electronic ground state and the single excited states have to be described on an atomic orbital basis for the theoretical evaluation of the electronic absorption behavior of molecules. Accurate calculations of molecular vertical excitation energies and the corresponding dipole moments are essential to analyze the electronic absorption spectra. Generating a qualitatively acceptable description of excited states is much more challenging task than the analogous ground-state calculations. This is because,

the ground-state electronic wavefunction is usually well approximated by a single Slater determinant, whereas much more complicated configuration interaction (CI) representations are often needed for the excited states [18]. Modern DFT calculations have proved highly successful at predicting the structures and electronic properties. In addition, TD-DFT calculations allow quantum chemists to probe the nature of excited states and facilitate a better understanding of observed electronic spectra.

The studied model comprised the monomer and dimer assemblies of liquid crystalline biphenylcyclohexane molecules BCH30 and BCH5CN. The general structural parameters of the systems such as bond lengths and bond angles have been taken from published crystallographic data [17]. Geometry optimizations have been performed using the DFT approach [13], and in particular, the Becke3-Lee-Yang-Parr hybrid functional (B3LYP), exchange-correlation functional, and the 6–31G (d) basis set. The DFT approach was originally developed by Hohenberg and Kohn [19], Kohn and Sham [20, 21] to provide an efficient method of handling the many-electron system. The theory allows us to reduce the problem of an interacting many-electron system to an effective single-electron problem. On the basis of the DFT geometries, the electronic structures, excitation energies, and excited wavefunctions have been calculated at a semiempirical Hartree–Fock level with the ZINDO/S method [22, 23] (Intermediate Neglect of Differential Overlap method, as parameterized by Zerner and co-workers) coupled with the CI single level of approximation including all $\pi \rightarrow \pi^*$ single excitations. This has been found adequate to determine the UV-Vis. absorption spectra [24, 25].

The DFT calculations have been performed by a spectroscopy oriented configuration interaction procedure (SORCI) [26]. The charge distributions of the molecules have been calculated by performing Mulliken population analysis and Loewdin population analysis. The mesomorphic behavior and the phase stability have been predicted through the calculated local charge distributions. Based on the optimal geometry obtained for each molecule, a systematic examination of interactions between a pair of isolated molecules has been carried out. The absorption maxima, HOMO, and LUMO orbitals have been analyzed to describe the electronic properties of the systems.

Results and Discussion

The geometric structures of BCH30 and BCH5CN have been shown in Fig. 1. The structures have been constructed on the basis of published crystallographic data with the standard values of bond lengths and bond angles [17]. In both the compounds, the molecules form layers in the crystalline state. The dihedral angles between the phenyl rings in the biphenyl unit are 2.4° in BCH5CN and 23.8° BCH30, respectively [17]. Mulliken and Loewdin atomic net charges have been calculated. The molecular charge distribution and phase stability of the molecules have been analyzed as given below.

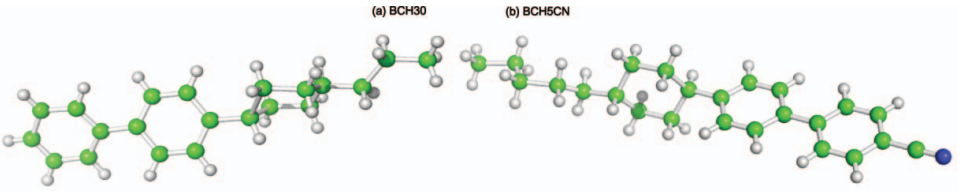

Figure 1. The geometric structures of (a) BCH30 and (b) BCH5CN molecules.

Molecular Charge Distribution and Phase Stability

It is expected that the specific charge distributions and electrostatic interactions in LC molecules play an influential role in the various mesophases. An appropriate modeling of this fundamental molecular facet relies on the possibility of assigning a partial charge to all atomic centers [2]. Analysis of molecular charge distribution can deliver good information about local electrostatic interactions, which is not possible from experimental point of view. To parameterize the molecular interactions for computational studies, atom-positioned partial charges are helpful [6]. Quantum chemical computations offer the possibility to take a detailed look at the electronic structure of the molecules. These charges represent the electrostatic molecular interactions very well, but they do not show the real charge distribution in the molecule.

The group charges are needed to explain the behavior of mesogens. The Mulliken population analysis has been performed for each molecule, and the atomic charges have been compared with Loewdin charges. However, there is much agreement among the methods while it comes to the group charges. It is evident from Table 1 that the positive-charged side group in BCH30 (C_3H_7) will be strongly attracted by the negative-charged core. Whereas, the presence of strong polar group (CN) in BCH5CN provides enough attractive force for the positive-charged large side group (C_5H_{11}) to maintain the thermodynamic stability. Ultimately, this causes the formation of longer units in the mesophase. Hence, the phase stability is expected to be high for BCH5CN. Further, the amplitude of thermal vibration of the side group carbon atoms increases markedly for BCH30 due to the positively charged terminal group (H). This indicates a low packing efficiency and phase stability that leads to a drastic decrease in phase transition temperature. The mesophase to isotropic transition temperature of the molecules reported by the crystallographer (Table 1) supports this finding.

Electronic Absorption Spectra

One of the most exciting developments in LC science and technology is the application of using light instead of electricity to control the behavior of a material [23, 24]. The description of molecular quantities by quantum chemical methods underlies some principle restrictions, i.e., there exists a compromise between the complexity of the systems studied and the accessible theoretical accuracy. For the calculation of electronic spectra, the CI method is widely employed. Using a CI method in combination with a semiempirical model Hamiltonian, an evaluation of absorption spectra of large organic molecules and LCs becomes possible [6, 9, 24, 25]. The principal absorption bands in the molecules are due to the $\pi \rightarrow \pi^*$ transitions in the benzene analogous part of the molecule. In general, these benzene-like transitions are roughly conserved in the model systems studied, but they are influenced by the conjugation length, degree of conjugation, and the different substituents.

Table 1. Mulliken (M), Loewdin (L) group charges and mesophase-isotropic transition temperatures for BCH molecules

	Side group		Core		Terminal group		
Molecule	M	L	M	L	M	L	T (K) [17]
BCH30	0.303	0.086	−0.386	−0.115	0.084	0.028	366 (S_B-I)
BCH5CN	0.461	0.241	−0.278	−0.071	−0.183	−0.170	494 (N-I)

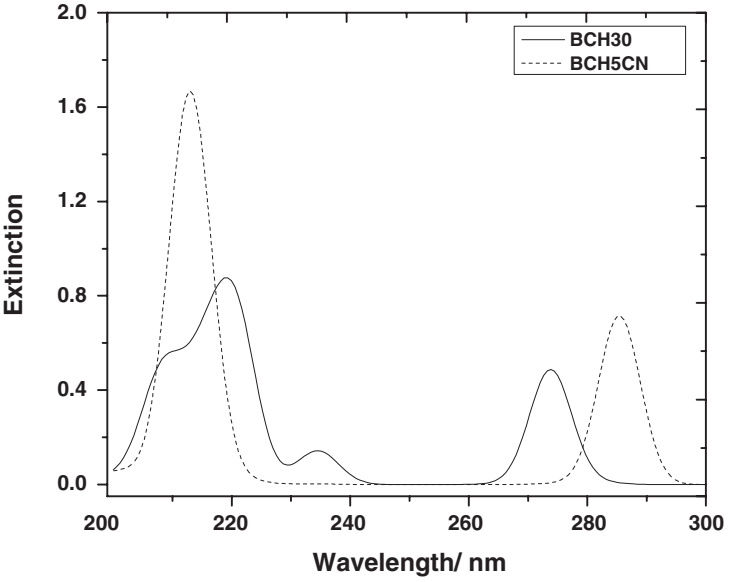

Figure 2. Electronic absorption spectra of BCH molecules. Extinction unit: 10^4 dm^3 mol^{-1} cm^{-1}.

The electronic absorption spectra of BCH30 and BCH5CN molecules have been shown in Fig. 2. The influence of the substituents in the aromatic core on the position of the absorption bands is evident from the spectral data. In the UV region, three strong absorptions at 219.34, 234.57, and 273.83 nm have been observed. However, no absorption has been observed in the visible region. The strongest band appears in a region from 200 nm to 229.88 nm with absorption maxima (λ_{max}) at 219.34 nm, with one shoulder at 212.3 nm. This band arises from the HOMO→LUMO transition, and is assigned as $\pi \rightarrow \pi^*$ transition in the molecule. Further, the calculations also predict two more $\pi \rightarrow \pi^*$ transitions corresponding to weak absorption bands at other two wavelengths. The absorption spectrum of BCH5CN molecule (Fig. 2) shows two prominent bands in the UV region with absorption maxima at 212.89 and 285.55 nm. The strongest band has been observed from 200 nm to 242.77 nm with absorption maxima at 212.89 nm. This band arises due to the HOMO→LUMO transition, and is assigned as $\pi \rightarrow \pi^*$ transition in the molecule. The other band also indicates the possibility of $\pi \rightarrow \pi^*$ transitions. Hence, both the molecules show a profound preference for $\pi \rightarrow \pi^*$ transition, which occur at lower wavelengths. The spectral data reveal that the substitution of different side groups causes a red-shift of absorption wavelength (for BCH30), and a decrement in transition energies (Table 2). This indicates a weak exciton coupling of chromophores, and it is due to an increase in dipole moment on excitation of the electron. This makes the band to interact more electrostatically, leads to a change in charge distribution, and an increased delocalization of electrons. Thus, both the ground and excited n→π^* transition does not occur due to the rigidity of the ring system of the molecules.

It is clear from the above discussion that the BCH30 system is exhibiting a higher symmetric representation. This is because a $\pi \rightarrow \pi^*$ transition is only possible, if the direct product of the ground state wavefunction, the excited one, and the dipole moment operator contains the totally symmetric representation. A more number of $\pi \rightarrow \pi^*$ transitions leads to a higher symmetric representation [25, 27]. The absorption wavelength is found to be high for BCH30 molecule with the more number of $\pi \rightarrow \pi^*$ transitions. Thus, the comparison of

Table 2. The extinction coefficients corresponding to absorption wavelength (λ_{max}), HOMO, LUMO energies, and energy gap (E_g) of BCH molecules

Molecule	λ_{max} (nm)		Extinction[a]		HOMO (eV)	LUMO (eV)	E_g = (LUMO-HOMO) (eV)
	UV-Vis.	CD	UV-Vis.	CD			
BCH30	219.34	208.20	0.88	87.79	−7.98	0.28	8.26
BCH5CN	212.89	222.27	1.67	16.46	−8.30	−0.39	7.91
Dimer molecules							
BCH30							
Stacking	200.00	212.89	1.19	47.84	−7.54	0.34	7.88
In-plane	294.92	204.69	1.24	371.23	−7.55	0.35	7.90
BCH5CN							
Stacking	301.95	200.00	1.16	131.13	−7.93	−0.29	7.64
In-plane	298.44	296.09	1.55	345.67	−7.96	−0.23	7.73

[a]Extinction unit: 10^4 dm^3 mol^{-1} cm^{-1}.

absorption maxima between BCH5CN and BCH30 indicates a bathochromic (red) shift (the shift of maximum absorption to a longer wavelength). Further, the transition probability is usually characterized by the oscillator strength, which is related to the integrated intensity of the absorption band. The extinction coefficients corresponding to absorption maxima, HOMO, LUMO energies, the energy gap (E_g) values of isolated molecules, and dimers have been reported in Table 2. The estimation of extinction coefficients from BCH30 to BCH5CN indicates a hyperchromic effect (increment in absorbance) as evident from Table 2. The absorption spectrum of BCH5CN in the UV region is identical to those of 4′-n-Pentyl-4-Cyanobiphenyl (5CB) [9] because of the identical π-electron structure [28]. The principal effects of cyclohexane ring to absorption are: (i) it contributes more σ-electrons to the molecule; (ii) it reduces the packing density due to the elongated molecular size. Thus, the overall electronic absorption may only slightly increase (Fig. 2). The up shift might be due to the diminution of the deshielding effect of the electron withdrawing (cyano) group, and the long alkyl spacer attached to the aromatic core. This may allow the molecule in resulting the observed hyperchromic effect. Further, the HOMO, LUMO, and the energy gap (E_{LUMO}–E_{HOMO}) values are high for BCH30 than BCH5CN. Due to the extended conjugation in BCH5CN, the HOMO and LUMO orbitals come closer, and the energy gap value decreases for BCH5CN (Table 2). Depending on the localization properties of the wavefunctions participating in the electronic transitions, the shifts in the absorption wavelengths have been found. These may be controlled and influenced by the position of the chemical substituents in the corresponding π systems.

Circular Dichroism (CD) Spectra

The CD spectra of BCH30 and BCH5CN molecules have been shown in Fig. 3. Three strong absorption bands in the UV region at 208.2, 234.57, and 273.83 nm have been observed. The strongest band appears in a region from 200 nm to 221.68 nm with absorption maxima at 208.2 nm. Further, two strong absorption bands have been noticed for BCH5CN (Fig. 3) at 222.27 and 285.55 nm. The strongest band appears in a region from 211.13 nm to 235.16 nm with absorption maxima at 222.27 nm.

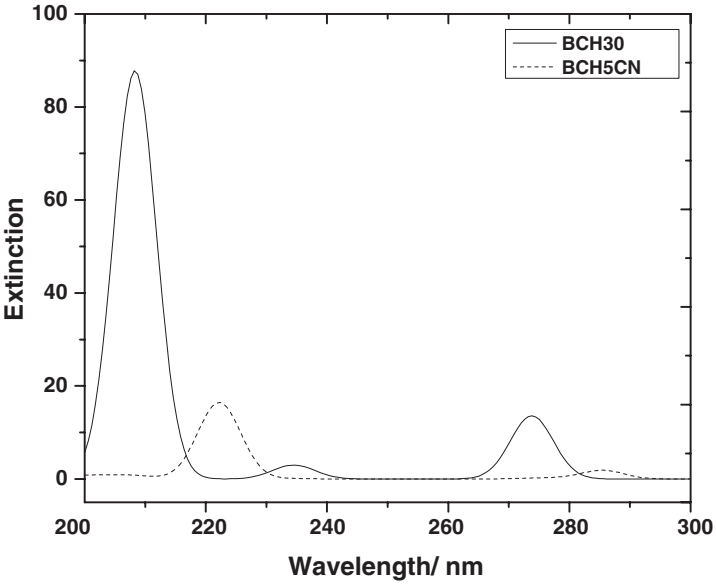

Figure 3. CD spectra of BCH molecules. Extinction unit: 10^4 dm^3 mol^{-1} cm^{-1}.

It may, therefore, be concluded that the absorption wavelength in CD spectrum shows a preference for BCH5CN. However, the substitution of alkyl groups and cyano group leads to a drastic decrease in the extinction coefficient. The maximum transition oscillator strength (f), rotatory strength (R), transition energies, the corresponding wavelengths for isolated molecules, and dimer complexes of BCHs at the TDDFT/B3LYP/6–31+G (d) level of approximation have been reported in Table 3. The wavelength dependence of oscillator strength (f) (Fig. 4) and rotatory strength (R) (Fig. 5) of BCHs molecules reveals that the molecule BCH5CN shows higher oscillator strength at lower wavelength as compared to BCH30. An important characteristic of molecules is the oscillator strength (f), which reveals the effective number of electrons whose transition from the ground to the excited state gives

Table 3. The maximum transition oscillator strength (f), rotatory strength (R), transition energies, the corresponding wavelengths for isolated molecules, and dimer complexes of BCH molecules at the TDDFT/B3LYP/6–31+G (d) level of approximation

Molecule	λ (nm)	f	Energy (cm^{-1})	Λ (nm)	R	Energy (cm^{-1})
BCH30	219.34	0.69	45,329.7	208.3	87.82	48,010.5
BCH5CN	212.89	0.97	46,843.1	222.2	16.46	44,999.3
Dimer molecules						
BCH30						
Stacking	200.00	0.87	33,792.6	293.7	93.69	34,048.0
In-plane	294.92	1.23	33,932.5	205.4	324.38	48,675.1
BCH5CN						
Stacking	301.95	0.98	32,978.6	206.9	96.43	48,335.5
In-plane	298.44	1.48	33,490.1	296.3	346.26	33,754.0

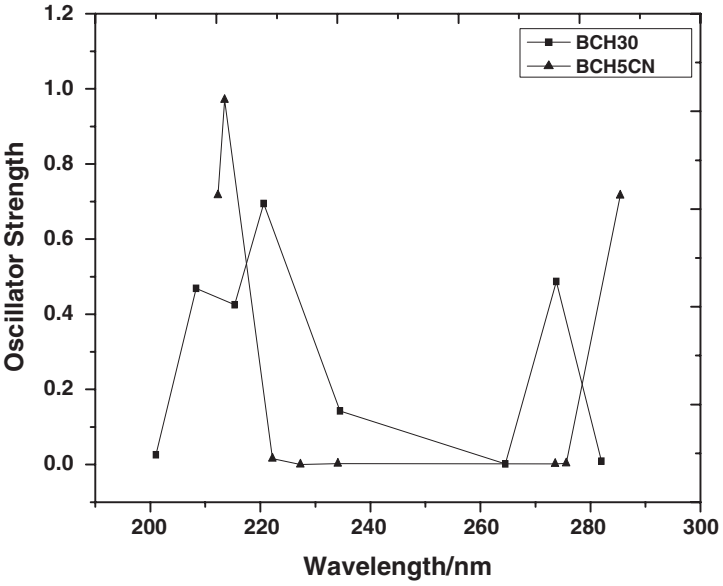

Figure 4. Wavelength dependence of oscillator strength (*f*) of BCH30 and BCH5CN.

the absorption area of the spectrum. The oscillator strength also indicates the allowedness of electronic transitions in a molecule. This implies that the molecule BCH5CN is more flexible for electronic transitions in UV range, as the molecule exhibits higher oscillator strength (Table 3). However, the molecule BCH30 shows higher rotatory strength at lower wavelength compared to BCH5CN. The comparison of absorption wavelength indicates

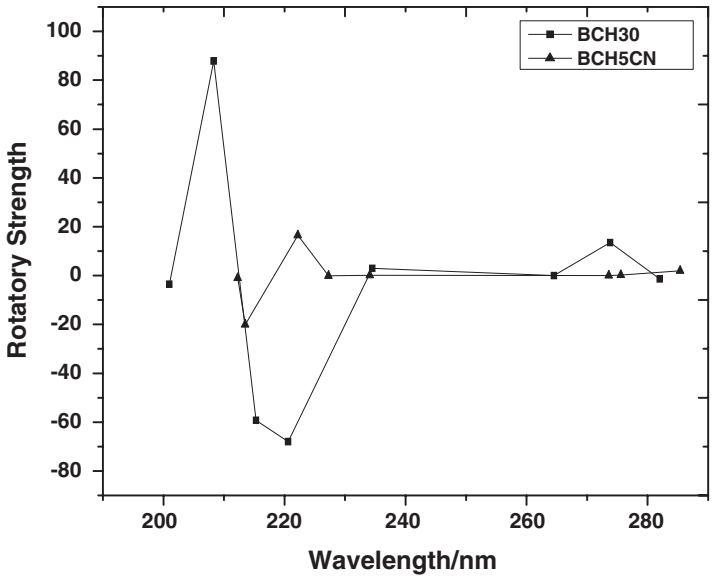

Figure 5. Wavelength dependence of rotatory strength (*R*) of BCH30 and BCH5CN.

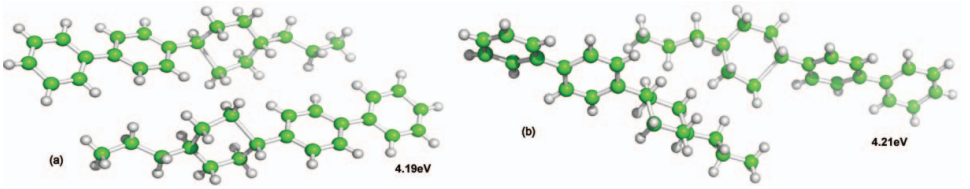

Figure 6. Energetically favorable structures of BCH30 dimers in (a) stacking and (b) in-plane interactions.

that BCH30 exhibits higher UV stability as its absorption wavelength is higher to BCH5CN (Table 2). Further, both the molecules exhibiting a constant oscillator/rotatory strengths in a particular UV wavelength range, which may be exploited for organic electronic applications.

Intermolecular Interactions Between Pair of Molecules

The results obtained for isolated molecules suggest that the electronic and optical properties have been influenced by their electronic structures. The self-assembly of suitable building blocks, through intermolecular interactions of different nature, is a current approach to design new LC materials. Therefore, to understand the self-organizing ability of mesogens, the different types of molecular interactions, viz., stacking and in-plane modes, have been taken into consideration between a pair of BCHs molecules. The interaction energies of dimer complexes have been taken to investigate the most energetically stable configuration in each mode. Further, the optical properties of dimer complexes have been reported in Table 2. LCs are not isotropic, and clearly, intermolecular interactions strongly influence their phase behavior/stability and properties. The interpretation of physical measurements on LCs in terms of molecular properties is, therefore, a difficult problem. Hence, the basic idea underlying the study of molecular conformations is to show the physical and chemical properties of compounds that are closely related to the preferred conformations. Moreover, the details of molecular and conformational structure are necessary for a deeper analysis of the relation between crystalline and LC states.

The conformational behavior of LCs displays a large variation in the intermolecular effects that depends on the nature and magnitude of interactions. Each conformation may have distinct energy, and lower energy conformations will be populated in preference to those of higher energy. The most energetically stable configurations of BCH30 and BCH5CN molecules during the different modes of interactions have been shown in Figs. 6 and 7, respectively. The comparison of dimers between both the molecules suggests that with the extension of the chain length, a recognizable segregation of the dimers into a

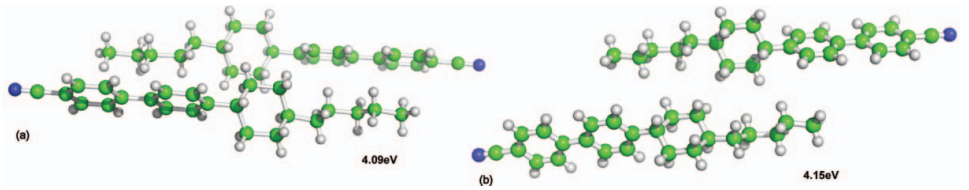

Figure 7. Energetically favorable structures of BCH5CN dimers in (a) stacking and (b) in-plane interactions.

highly tilted layer structure has been obtained for BCH5CN molecule (Fig. 7). The mutual interaction between the dimers in this structure is, however, quite weak in particular to chain atoms. Hence, the end chains provide enough disorder to the crystal to pass on to nematic rather than smectic phase. This is due to the fact that the probability of thermal fluctuations as well as the occurrence of different conformations increases as the alkyl chain becomes longer. The comparison of interaction energy values for both the molecules indicates that the BCH5CN dimers are more stable and, hence, causing high phase stability.

Conclusions

The salient features of the present work are:

1. The electronic absorption and CD spectra of liquid crystalline biphenylcyclohexane molecules show strongest absorption band due to the transition between HOMO→LUMO energy states that can be assigned as $\pi \rightarrow \pi^*$ transitions. However, the appearance of other bands also indicate the possibility of additional $\pi \rightarrow \pi^*$ transitions.
2. A red-shift of absorption wavelength and a decrement in excited energies for BCH30 indicates a weak exciton coupling of chromophores. This is due to an increase in dipole moment on excitation of the electron. This makes the band to interact more electrostatically, leads to a change in charge distribution, and an increased delocalization of electrons. Thus, both the ground and excited $n \rightarrow \pi^*$ transition does not occur due to the rigidity of the ring system of the molecules.
3. The molecule BCH5CN shows higher oscillator strength at lower wavelength as compared to BCH30. However, the molecule BCH30 shows higher rotatory strength at lower wavelength compared to BCH5CN molecule. Further, BCH30 exhibits higher UV stability than BCH5CN molecule.
4. Due to the extended conjugation in BCH5CN, the HOMO and LUMO orbitals come closer, and the energy gap value decreases for BCH5CN molecule (Table 2).
5. Due to the extension of the chain length, a recognizable segregation of the dimers into a highly tilted layer structure has been obtained for BCH5CN. The mutual interaction between the dimers in this structure is, however, quite weak, in particular to chain atoms. Hence, the end chains provide enough disorder to the crystal to pass on to nematic rather than smectic phase. Further, interaction energy values for both the molecules indicate that the BCH5CN dimers are more stable and, hence, causing high phase stability. This supports the finding from charge distribution analysis.

Acknowledgments

The financial support rendered by the Council of Scientific and Industrial Research (CSIR) and University Grants Commission (UGC), New Delhi, India is gratefully acknowledged.

References

[1] Zhang, Z., & Guo, H. (2010). *J. Chem. Phys.*, *133*, 1–12.
[2] Lakshmi Praveen, P., & Ojha, D. P. (2011). *Mat. Chem. Phys.*, *126*, 248–252.
[3] Nazarenko, V. G., Boiko, O. P., Anisimov, M. I., Kadashchuk, A. K., Nastishin, Yu. A., Golovin, A. B., & Lavrentovich, O. D. (2010). *Appl. Phys. Lett.*, *97*, 1–3.
[4] Liu, Y., Zhan, G., Zhong, X., Yu, Y., & Gan, W. (2011). *Liq. Cryst.*, *38*, 995–1006.

[5] Frunza, L., Frunza, S., Zgura, I., Beica, T., Gheorghe, N., Ganea, P., Stoenescu, D., Dinescu, A., & Schönhals, A. (2010). *Spectrochim. Acta A*, *75*, 1228–1235.
[6] Lakshmi Praveen, P., & Ojha, D. P. (2011). *Liq. Cryst.*, *38*, 963–970.
[7] Peroukidis, S. D., Vanakaras, A. G., & Photinos, D. J. (2008). *J. Phy. Chem. B.*, *112*, 12761–12767.
[8] Yilmaz, S., & Bozkurt, A. (2008). *Mat. Chem. Phys.*, *107*, 410–412.
[9] Lakshmi Praveen, P., & Ojha, D. P. (2011). *Phys. Rev. E*, *83*, 1–7.
[10] Otani, T., Araoka, F., Ishikawa, K., & Takezoe, H. (2009). *J. Am. Chem. Soc.*, *131*, 12368–12372.
[11] Priimägi, A., Kaivola, M., Rodriguez, F. J., & Kauranen, M. (2007). *Appl. Phys. Lett.*, *90*, 1–3.
[12] Dalton, L. R., Harper, A. W., & Robinson, B. H. (1997). *Proc. Nat. Acad. Sci.*, *94*, 4842–4847.
[13] Koch, W., & Holthausen, M. C. (2000). *A Chemist's Guide to Density Functional Theory*, Wiley-VCH: Weinheim.
[14] Peng, H. L., Payton, J. L., Protasiewicz, J. D., & Simpson, M. C. (2009). *J. Phys. Chem. A*, *113*, 7054–7063.
[15] Grabchev, I., & Chovelon, J. M. (2003). *Z. Naturforsch.*, *58a*, 45–50.
[16] Chen, Q., Sargent, E. H., Leclerc, N., & Attias, A. J. (2003). *Appl. Opt.*, *42*, 7235–7241.
[17] Haase, W., Paulus, H., & Muller, H. T. (1983). *Mol. Cryst. Liq. Cryst.*, *97*, 131–147.
[18] Szabo, A., & Ostlund, N. S. (1989). *Modern Quantum Chemistry: Introduction to Advanced Electronic Structure Theory*, McGraw-Hill: New York.
[19] Hohenberg, P., & Kohn, W. (1965). *Phys. Rev.*, *537*, B864–B871.
[20] Kohn, W., & Sham, L. J. (1965). *Phys. Rev.*, *140*, A1133–A1188.
[21] Jones, R. O., & Gunnarsson, O. (1989). *Rev. Mod. Phys.*, *61*, 689–746.
[22] Zerner, M. C. (1991). *Rev. Comp. Chem.*, *2*, 313–365.
[23] Zerner, M. C. (2004). In: K. W. Lipkowitz, R. Larter, & Th. R. Cunsari (Eds.), *Semiempirical Molecular Orbital Methods*, Wiley-VCH: New Jersey, p. 153.
[24] Hanemann, T., Bohm, M. C., Haase, W., & Wu, S. T. (1992). *Liq. Cryst.*, *11*, 917–927.
[25] Quotschalla, U., Hanemann, T., Bohm, M. C., & Haase, W. (1991). *Mol. Cryst. Liq. Cryst.*, *207*, 103–116.
[26] Neese, F. A. (2003). *J. Chem. Phys.*, *119*, 9428–9444.
[27] McConnell, H. (1952). *J. Chem. Phys.*, *20*, 700–704.
[28] Khoo, I. C., & Wu, S. T. (1993). *Optics and Non Linear Optics of Liquid Crystals*, World Scientific: Singapore.